Journal of Hydrology 546 (2017) 219–229

Contents lists available at ScienceDirect

Journal of Hydrology

journal homepage: www.elsevier.com/locate/jhydrol

Research papers

Water fluxes between inter-patches and vegetated mounds in flat semiarid landscapes

María J. Rossi *, Jorge O. Ares

National Patagonic Centre, National Council for Scientific and Technological Research, Argentina (CONICET), Puerto Madryn, Argentina

ARTICLE INFO

Article history:
Received 1 September 2016
Received in revised form 9 November 2016
Accepted 10 January 2017
Available online 16 January 2017
This manuscript was handled by Corrado Corradini, Editor-in-Chief, with the assistance of Rao S. Govindaraju, Associate Editor

Keywords:
Infiltration
Runoff
Vegetated mound
Preferential infiltration
Soil micro-topography

ABSTRACT

It has been assumed that bare soil (BS) inter-patches in semi arid spotted vegetation behave as sources of water to near vegetated soil (VS) patches. However, little evidence has been gained from direct measurements of overland and infiltration water fluxes between bare soil inter-patches and shrub mounds at a scale compatible with available high resolution imagery and hydrological modeling techniques. The objective of this study is to address the thin scale internal redistribution of water between BS inter-patches and vegetated mounds at relatively flat spotted semiarid landscapes. The relation between plant cover, topography and runoff was inspected with non-parametric association coefficients based on high resolution remotely sensed imagery, ground truth topographic elevation and spatial-explicit field data on potential runoff. Measurements of advective flows at the same spatial scale were carried out at micro-plots of BS and shrub mounds. Water fluxes between BS inter-patch and a shrub mound were simulated under varying typical Patagonian rainfall scenarios with an hydrological model. Results obtained revealed that the soil properties, infiltration and overland flow metrics at the mounds and inter-patches exhibit spatially and dynamic variable hydraulic properties. High micro-topographic roughness and depression storage thickened overland flow depth at VS patches. At BS inter-patches prevailing low slopes and depression storage were found to be important variables attenuating the surface runoff. At both rainfall scenarios simulated, the soil under the shrub mound accumulated more moisture (from direct rain) and reached saturation long before this occurred in BS nearby inter-patch area. Overland flow at the inter-patch was attenuated as it reached the border of the patch, diverging from the latter as it followed the (small) topographic gradient. The overland flow generated inside the vegetated mound was effectively retained at the typical Summer rainfall scenario; while several threads of runoff were routed outside the mound at the typical Winter rainfall scenario. The results here shown fail to detect: (a) enough runoff momentum that could route runon onto the vegetated mounds and (b) a contrast in infiltration rates between BS and the vegetated mound enough to lead to a free-surface gradient in ponded water that could inundate the mound.

1. Introduction

In many arid and semiarid environments around the world landscapes display a contrasting mosaic of areas occupied by individual shrubs, tussocks or groves of plants (with high biomass cover) interspersed with bare soil (BS) or low vegetation cover (Saco et al., 2007). The chemical, structural and textural properties of vegetated soil (VS) at the patches of plants are usually markedly different from those at the surrounding BS inter- patches (Dunkerley and Brown, 1995; Puigdefábregas et al., 1999; Bochet et al., 2006; Mayor et al., 2008; Liu et al., 2013b).

Many studies have hypothesized that the process of redistribution of water via overland flow, also known as runon, is caused by patchy vegetation in semiarid ecosystems. Redistribution occurs when overland flow generated in the BS inter-patch areas infiltrates under vegetation canopy where infiltration capacity is high. This hypothesis builds on the observation that the dynamics of both Hortonian (infiltration excess runoff) and Hewlettian (saturation excess overland flow) runoff vary between vegetated patches and inter-patches (Muñoz-Robles et al., 2011; Liu et al., 2013a) and that inter-patches commonly have lower infiltration capacity than vegetated patches (Bromley et al., 1997; Cerdá, 1997; Cammeraat and Imeson, 1999; Bochet et al., 2000; Wu et al., 2016) although opposite trends have also been reported (Nicolau et al., 1996; Caldwell et al., 2008).

* Corresponding author.
E-mail address: rossi@cenpat-conicet.gob.ar (M.J. Rossi).

http://dx.doi.org/10.1016/j.jhydrol.2017.01.016
0022-1694/

Acronyms

ANN	Artificial Neural Net
BS	Bare Soil
DEM	Digital Elevation Map
PCM	Plant Cover Map
PGI	Panchromatic Grey Intensity
PRM	Potential Runoff Map
PTFs	Pedotransfer functions
RP	Runoff Plume
TDI	Tension Disk Infiltrometer
TDR	Time-Domain Reflectometer
VS	Vegetated Soil

Variables [Units]

$A(t)$	instantaneous runoff plume area [mm^2]
C	friction coefficient
$ç^*$	mean runoff coefficient
ff	Darcy-Weisbach friction factor
Q_o	water stored at the runoff plume as overland flow [mm^3]
d^*	average water depth of the RP [mm]
DS	depression storage [% (Base: Total RP area)]
$f(t)$	time variable infiltration rate [mm s^{-1}]
$IN(t)$	instantaneous total infiltration flow [mm^3 s^{-1}]
K_{sat}	saturated hydraulic conductivity [mm s^{-1}]
L	parameter of soil structural tortuosity
m	terrain slope of the RP [mm]
$Q_o(t)$	time variable overland flow [mm^3 s^{-1}]
Q_v	water infiltrated at the upper vadose zone [mm^3]
R	rain depth [mm h^{-1}]
Re	Reynolds number
$s(t_{n+1}, t_n)$	average height drop along the contour of $A(t)$ at each time interval (t_{n+1}, t_n) [mm]
s^*	average $s(t_{n+1}, t_n)$ at the end of water flow experiment [mm]
$s°$	average slope of the plot
SBD	soil bulk density [g cm^{-3}]
SG	gravel content in soil [% (Base: Weight of dry (105°), sieved (2 mm mesh) soil)]
SR	amount of roots in soil [% (Base: Weight of dry (105°), sieved (2 mm mesh) soil)]
SS	sand content in soil [% (Base: Weight of dry (105°), sieved (2 mm mesh) soil)]
$V_{(s,\ W)}$	normalized RP velocity per unit height drop and water inflow [mm^3 s^{-1}]
v^*	average overland flow velocity during water flow experiment [mm s^{-1}]
W	water inflow rate [mm^3 s^{-1}]
θ_g	fraction of volumetric soil moisture
θ_h	soil moisture depth [mm]
θ_v	fraction of volumetric soil moisture
σ_s	surface roughness of the ground calculated as the standard deviation of $s(t_{n+1}, t_n)$ [mm]
υ	kinematic viscosity [mm^2 s^{-1}]

Much research on water redistribution has been conducted at large scales in semiarid regions with banded vegetation and mulga environments (Cornet et al., 1992; Bromley et al., 1997; Ludwig et al., 1999; Dunkerley, 2002; Moreno-de las Heras et al., 2012). In these regions it has been shown using soil moisture depth observations, manipulation of runoff, and computer simulations; that during rainstorms, patches of vegetation serve as surface obstructions that slow and trap runon, sediments, and nutrients from open inter-patch areas. Nevertheless, knowledge is rather poor about the thin scale water fluxes in patchy, non-banded vegetation, which is often structured in a spotted configuration associated with mounds (Wilcox et al., 2003; Ludwig et al., 2005; Li et al., 2008).

In spotted semiarid landscapes with absence of mound effects, water infiltrates faster into vegetated patches than into BS surface, which leads to a net displacement of surface water to vegetated patches (Cerdá, 1997). However, in spotted semiarid landscapes patchy vegetation often sits upon micro-topographic mounds (Bochet et al., 2000; Bedford and Small, 2008) which may partially obstruct overland flow paths. The potential energy gradients that drive overland flow at these sites can arise either from the topographic slope of the soil surface, or, in the absence of slope, from gradients in the free water surface (Appels et al., 2016).

There is a need for work involving studies aimed to understand the water transport processes at BS inter-patches and shrub mounds at spotted semiarid regions, specially involving direct measurement of water fluxes (Thompson et al., 2011; Harman et al., 2014). Some studies that take into account the effects of the shrub mounds (and associated micro-topographic properties) on water infiltration and overland flows at patchy semiarid regions are based solely on modeling approaches (Thompson et al., 2011; Chen et al., 2013; Chu et al., 2013; Liu et al., 2013a; Frei and Fleckenstein, 2014).

Other studies do not take due account of the effect of infiltration on advective flows by simulating dryland soil surfaces with technical artifacts (Dunkerley, 2003), or recreating flume experiments at laboratory conditions with uniform infiltration conditions (Strohmeier et al., 2014). Some studies at semiarid patchy landscapes involve the collection of runoff water samples taken at the outlet of plots composed by both vegetated and BS or/and a combination of these (Li et al., 2008; Reid et al., 1999; Rodríguez-Caballero et al., 2014). This latter technique, although efficient to prove that more rain is directly infiltrated into the VS and runoff is generated very quickly on BS; does not address water flow transport processes between BS inter-patches and shrub mounds. Even more, through these methods no field evidence is generated to study the role of surface roughness at the shrub mounds, which could impede lateral redistribution from surrounding BS, or at least confine redistribution strongly to the edges of the vegetated mounds (Thompson et al., 2011).

Vegetated mounds seem to be formed, developed and maintained by different processes: differential erosion (Rostagno and Del Valle, 1988) and/or the trapping of resources by vegetated clumps (Deblauwe et al., 2011; Wu et al., 2016). The latter consists on a "nucleation" process; a process of sequential scour (at BS) and deposition (at VS) by rainflow, sheetwash or rill erosion; and has been hypothesized as the main genesis and maintenance mechanism for banded vegetation (Bryan and Brun, 1999; Deblauwe et al., 2011). However, mound formation and maintenance at spotted Patagonian semiarid landscape has been attributed to splash and wash erosion processes (Rostagno and Del Valle, 1988). According to this hypothesis, the combination of rain-splash and overland flow would have eroded the BS areas, leaving pedestals or mounds protected by shrubs.

Results of a previous fine spatial scale (1–2 m) study (Rossi and Ares, 2016) at the Patagonian Monte indicate that overland flow can occur from the spotted vegetated mounds to the surrounding BS under certain circumstances. According to those, overland flow can transport resources (water, litter, nutrients, sediments, seeds)

from the relatively rich patch areas to the nearby soil. It was raised that there is a need to study the implications of this phenomenon in the surface distribution of water during typical storm events considering not only the vegetated mound water flows, but also the flows occurring at BS inter-patches and their interaction.

The objective of this study is to address the thin scale internal redistribution of water between BS inter-patches and vegetated mounds at relatively flat spotted semiarid landscapes. It is hypothesized that runon water may not be infiltrated in the shrub mounds at relatively flat spotted semiarid landscapes. Specifically: (a) the low topographic slopes at the BS inter-patches may not be enough to create the gradients of potential energy required to route overland flow onto the vegetated mounds; (b) high plant cover at the spotted vegetated mounds effectively retain overland flow generated at the vegetation patch; and (c) the spatial permeability contrasts (contrast in infiltration rate) between BS and the vegetated mound that could generate differences in the ponded depth between them and a free water surface may not be sufficient to inundate the mounds at typical Patagonian storms. These hypothesis were inspected with a set of field flow experiments, analysis of high resolution imagery and fine scale hydrological modeling were conducted.

To our knowledge, the study here presented is novel in combining field and model studies that simultaneously take into account coupled infiltration (including preferential infiltration induced by plant roots) and overland flow, micro-topography; vegetation cover and geomorphology to study the internal redistribution of water flows (internal hydrological dynamics) at BS inter-patches and vegetated mounds at relatively flat spotted semiarid landscapes.

2. Materials and methods

2.1. Study area

The Patagonian Monte shrubland occupies an area of 42,000 km^2 and is dominated by a spotted shrubland of *Larrea divaricata* and *Stipa* spp. (Ares et al., 1990; Bertiller et al., 1991). The local vegetation covers about 40–60% of the soil in a random patchy structure with three vegetation layers: the upper layer (1–2 m height) dominated by tall shrubs (*Larrea divaricata*, Schinus johnstonii Barkley, *Chuquiraga erinacea* Don., Atriplex lampa Gill. ex Moq., and *Lycium chilense* Miers ex Bert.), the intermediate layer (0.5–1.2 m height) also composed by dwarf shrubs (*Nassauvia fuegiana* (Speg.) Cabrera, *Junellia seriphioides* (Gillies and Hook) Mold., and *Acantholippia seriphioides* (A. Grey) Mold.), and the low layer (0.1–0.5 m height) dominated by perennial grasses (*Nassella tenuis* (Phil.) Barkworth, *Pappostipa speciosa* (Trin. and Rupr.) Romasch, and *Poa ligularis* (Nees ex Steud)) (Ares et al., 1990; Carrera et al., 2008).

The study and experiments here presented were performed at two representative sites of the Patagonian Monte (Argentina), which is a temperate region with a Mediterranean-like rainfall regime (Abraham et al., 2009). The mean annual temperature is 13.4 °C and the long-term (1995–2004) average annual precipitation is 236 mm, although a recent study reports below and well above mean anual precipitation values (221.8 mm at 2012 and 354.6 mm at 2013) (Campanella et al., 2016). At the cold semiarid Patagonia, rainfall is irregularly distributed throughout the year. Long light winter and fall precipitation prevails (Mazzonia and Vazquez, 2009), with 70% of annual rainfall occurring in these seasons (Sala et al., 1989). Heavy (and shorter) rainfall events are more common during the warm season.

Site A (UL corner: S: −42.516477, W: −64.742319; LR corner: S: −42.516879, W: −64.741796) was selected for a study coupling high resolution (0.6 m) remotely sensed imagery of vegetation patches and the effects of mound scale topography on runoff (Section 2.2). Site B (UL corner: S: −42.16972, W: −64.9934; LR corner: S: −42.2144, W: −64.96193), a 4.8 km north-eastern-facing slope transect, was selected for water flow experiments at a thin (1 m) spatial scale (Section 2.3).

In both sites, A and B, soils are a complex of Typic Petrocalcids–Typic Haplocalcids with a fractured calcium carbonate layer from 0.45 to 1 m below the soil surface (del Valle et al., 1998). Upper soil texture types (USDA) are sandy or loamy sand (Rossi and Ares, 2012a) and volumetric soil moisture at field capacity is c.a. 25% (Bisigato and Bertiller, 1999; Rostagno et al., 1991).

2.2. Vegetation-topography-runoff interactions

An altimetry survey was conducted at a field-plot (300 × 239 m) at site A, by means of a high precision geodetic GPS receiver (LT400HS, CHC, Shangai). The elevation was surveyed at 3388 ground points spaced at 0.52 ± 0.005 m. These data were processed (kriging interpolation) by geo-statistical modeling tools (Surfer v. 7, Golden Software Inc., Colorado) to construct a DEM of 1 m spatial resolution. A Potential Runoff Map (PRM) was built based on the DEM through an 8-cell algorithm (Jenson and Domingue, 1988) (RUNOFF module, Idrisi v. 14.02 (Clark Labs, Worcester).

A Plant Cover Map (PCM) of the area was constructed by means of a QuickBird satellite (Catalog-Date: 10100100033BBB00-09/07/04) high resolution (0.6 m) panchromatic band (Fig. 1a). In this type of images, plant patches appear as spots-clumps of varying Panchromatic Grey Intensity (PGI) depending on the extent and aggregation of plant cover; high values (white-rich) corresponding to areas of BS or sparse grass-shrub cover, low values (black-rich) corresponding to dense shrubby-grass areas (Ares et al., 2003). A central plot in the image (30 × 30 m) with 0.02° topographic general slope was selected for detailed analysis of the relations vegetation-topography-runoff. The PGI was re-scaled (range: 0–128) and cross-tabulations (CROSSTAB, Idrisi v.14) of the digitized DEM × PCM and PRM × PCM were performed. Cramér-von Mises non parametric association (Stephens, 1970) analyses were performed on the obtained tables.

2.3. Field sampling and experiments

2.3.1. Sampling and measurement of soil properties

Soil properties were sampled at 60 cores (Ø: 40 mm, 0–18 cm depth) in inter-patches (35) of BS and patches (25) of VS, located in the site B; a field representative of the semiarid Patagonian Monte. BS inter-patches were not strictly of denuded soil, but rather those where bare soil accounted for >98% of the area. At

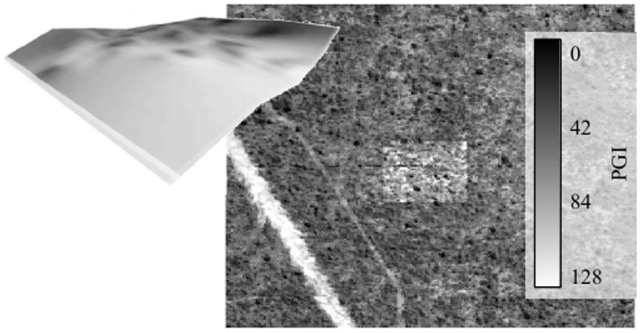

Fig. 1. A section of the QuickBird satellite panchromatic band (resolution: 0.6 m) image of the area and study plot (center) at site A and a fly-through view of its 1 m spatial resolution altimetry map (left).

least one well-developed plant patch was present in VS conditions, which also included part of a neighbor bare soil inter-patch. Both BS and VS conditions were selected in varying situations corresponding to mound types and sizes, depressions and slope classes.

Soil bulk density (*SBD*) was measured through the excavation method (ISO 11272, 1998). Undisturbed soil cores were extracted, brought to the laboratory in sealed containers and used to estimate gravimetric moisture (θ_g) and the corresponding volumetric (θ_v) equivalent through correction with soil bulk density.

Roots (*RS*) and gravel (*SG*) at VS samples were separated from the soil by sieving through a 2 mm mesh, washed, dried at 70 °C for 48 h, and weighed (Böhm, 1979). The texture (*SS*) of the sieved soil core samples was characterized with Lamotte's 1067 texture kit (LaMotte Co., Chestertown) calibrated with replicate estimates obtained at two reference laboratories (National Patagonic Centre, National University of the South, Argentina) with the Robinson's protocol (Gee and Bauder, 1986). Parameters corresponding to residual volumetric moisture (θ_r), saturated moisture content (θ_{sat}), K_{sat}, tortuosity connectivity (L), and shape of the soil moisture-water head function ($\log_{10}\alpha$, $\log_{10} n$) (van Genuchten, 1980) corresponding to the obtained soil samples were estimated based on textural data through Artificial Neural Net (ANN) pedotransfer functions (PTFs, Rosetta v. 1.2, US Salinity Laboratory, Riverside) developed by Schaap and Leij (1998).

Significant differences ($P \leqslant 0.05$) between properties of the soil samples under BS and VS conditions were determined using Student's *t*-tests.

Infiltration tests to obtain time-varying infiltration curves were performed using a Tension Disk Infiltrometer (TDI), (Ø: =45 mm, Decagon Devices, Pullman, WA). Test infiltration surfaces in the neighborhood of each plot were prepared by adding a 3 mm layer of silica sand (0.1–0.5 mm grain diameter) on the soil surface to improve hydraulic contact between the soil and the infiltrometer Disk. K_{sat} was estimated through Wooding's (1968) model:

$$f(t_\infty) = K_{sat}\left[(1 + 4/(\alpha.\pi.r))e^{(\alpha.h)}\right] \quad (1)$$

where $f(t_\infty)$ is the steady state infiltration rate at the TDI working tension h (mm s^{-1}), α is the inverse of the air-entry (kPa^{-1}) value estimated through ANN PTFs and r is the TDI disk radius (mm).

Steady infiltration rates were calculated by fitting an exponential curve (TableCurve 2D v.5.01, Systat Software Inc., San Jose, California) to the sequence of $f(t)$ data at 30-second intervals, where:

$$f(t) = a + bx^c \quad (2)$$

where $f(t)$ is the instantaneous infiltration rate (mm s^{-1}) and $a = f(t_\infty)$.

2.3.2. Water flow experiments

Water flow experiments were carried on 13 BS and 12 VS plots (0.8 × 0.8 m) regularly spaced along a transect described in Section 2.3.1 comprising a variety of depressions and vegetated mound conditions. A high precision DEM of each plot with *x-y-z* resolution ⩽2 mm was constructed through a close-range stereophotogrammetry and geo-statistical procedure (Rossi and Ares, 2012b). The procedure included obtaining a cenital color photograph (Kodak EasyShare Z712 IS 7.1 MP, Rochester) of the plots, taken at +50 cm above the soil surface.

The method used to create water flows connecting VS-BS areas did not intend to reproduce natural rainfall conditions but to create water head gradients at specific points in inter-patches and mounds as separated but interrelated units. Water was supplied during varying time intervals (11–19 min) at rates 13.5–26.5 mm min^{-1} with a single nozzle on a small area (2.5–12.2 cm^2) until the Runoff Plume (RP) reached some border of the BS plots. In VS plots, water inflow was always centered on the plant patch and the RP was observed until it reached the border of the vegetated patch. The selected water inflow rates were aimed to simulate flow accumulation values at the spatial scales of this study as estimated with a flow routing algorithm. This involved the definition of flow directions by D8 algorithm and flow accumulation as the accumulated weight of all cells flowing into each downslope cell in the output raster (Tarboton, 1997). All overland flow was infiltrated within the plot areas at the end of the experiments.

The antecedent and post-inflow volumetric soil (depth: 0–30 mm) moisture (θ_v) were estimated by means of a TDR (Time-Domain Reflectometer, TRIME®-FM, Ettlingen) pin probe (50 mm) at equidistant (30–35 mm) points of a grid covering the whole RP area and neighbor dry points. TDR estimates were calibrated with an independent set of gravimetric soil moisture measurements. The gravimetric moisture was assessed immediately after the water inflow ceased by extracting 2–5 soil cores (Ø: 40 mm, depth: 0–30, 31–60, 60–150 mm) along the main axis of the RP area.

The RP areas were video-recorded and video scenes were selected at specific time intervals (1 to 4 min, depending on the total duration of the experiments), exported to an image processing application (Idrisi v. 14.02, Clark Labs, Worcester), orthorectified, and overlaid to their corresponding DEM. The following metrics of the RPs were estimated:

- *DS*: Part of the RP area where depression storage occurs (%)
- $s°$: average slope of the plot (°)
- $s(t_{n+1}, t_n)$: average height drop along the contour of the runoff plume area ($A(t)$) at each time interval (t_{n+1}, t_n) (mm)
- s^*: average $s(t_{n+1}, t_n)$ at the end of the water flow experiment (mm)
- v^*: average overland flow velocity during the water flow experiment (mm s^{-1})
- σ_s: surface roughness of the ground calculated as the standard deviation of $s(t_{n+1}, t_n)$ (mm)

$$\sigma_s = \sum_{t=1}^{t=end} (s_t - s^*)^2 / n \quad (3)$$

where s_t is the height drop along the contour of the runoff plume area at time t (mm).

A computer code was written to solve a system of ordinary differential equations to calculate the water mass-balance of coupled infiltration and overland flows and dynamic flow metrics (Rossi and Ares, 2012a, 2016) which are usually estimated in overland flow studies (Abrahams et al., 1990; Parsons et al., 1994; Dunkerley, 2001) in order to ease comparisons with reported data obtained at coarser spatial scales. The set of non-linear ordinary differential and continuity equations with time variable parameters representing the changes in storages of overland water and at the upper vadose zone are:

$$dQo/dt = W(t) - IN(t) - Qo(t) \quad (4)$$

$$dQv/dt = IN(t) \quad (5)$$

$$CW = Qo + Qv = \sum_{t=1}^{t=end} W(t) \quad (6)$$

were Q_o is the water stored at the runoff plume as overland flow (mm^3); Q_v is the water infiltrated at the upper vadose zone (mm^3), $IN(t)$ is the instantaneous total infiltration flow (mm^3 s^{-1}) and $Q_o(t)$ is the instantaneous overland flow (mm^3 s^{-1}).

2.3.3. Overland flow metrics

The depth d (mm) of the overland flowing water volume at time t (mm) was calculated with Darcy's general form of frictional law (Dingman, 2007; Mügler et al., 2011):

$$d(t) = (W/C)^2/s(t, t+1) \quad (7)$$

where the velocity term is replaced in this case with the water inflow rate W ($mm^3\ s^{-1}$) and C is a friction coefficient estimated through inverse modeling of the continuity equations of water flow (Rossi and Ares, 2012a).

$$c^* = (\Sigma_{t=1,n}(Q_o(t)/W)/n \quad (8)$$

where $ç^*$ is the mean runoff coefficient and $Q_o(t)$ is the overland flow ($mm^3\ s^{-1}$).

$$V_{(s,W)} = v^*/(s^*.W) \quad (9)$$

where V(s,W) (mm^{-3}) is a normalized RP velocity per unit height drop and water inflow.

$$Re = 4.v^*.d^*/\upsilon \quad (10)$$

where Re is the dimensionless Reynolds number, d^* is the time average of $d(t)$ and υ is the kinematic viscosity of the fluid, (0.9 $mm^2\ s^{-1}$).

The Darcy-Weisbach friction factor (ff) (Nakayama and Boucher, 1998) was estimated as:

$$ff = 64/Re \quad (11)$$

2.3.4. Spatial-explicit simulation of flow experiments

The interaction of differential infiltration rates, soil micro-topography, soil hydraulic conductivity and overland water flows (speed, friction) under varying rainfall situations were simulated with a version of the CREST model calibrated "*in situ*". A subset of results of the field flow experiments were used to calibrate at a fine spatial scale (<1 m) the CREST (Coupled Routing and Excess Storage) hydrological model (Wang et al., 2011) (See Supplementary Data 1). The model simulates the spatio-temporal variation of atmospheric, land surface and subsurface water fluxes and storages by field cell-to-cell simulation.

The input parameters to CREST model (infiltration, soil micro-topography, soil hydraulic conductivity, depression storage and overland flow metrics) were estimated through sampling of the soil properties at the field and the overland flow experiments (Section 2.3). Stemflow water flux within the plant patch was estimated as in Rossi and Ares (2016). The CREST model outputs (overland flow paths-depths, soil moisture depths) were digitized with the Idrisi (v. 14.02, Clark Labs, Worcester) application to ease visualization.

3. Results

3.1. Vegetation-topography-runoff interactions

Fig. 1 shows a section of the QuickBird satellite panchromatic band (resolution: 0.6 m) image of the area and study plot at site A and a fly-through view of its 1 m spatial resolution altimetry map. The results of the cross-tabulation DEM × PCM (Fig. 2a) show moderate evidence (0.1 < Cramer's V < 0.3) that very dense shrubs (PGI: 0–20) are not very frequent at the study site (less than 0.005), but the two peaks of frequency are concentrated at the mound altitudes: 27 and 39 cm above the general slope level. Dense (PGI: 21–40) and shrubby-grass areas (PGI: 41–60) are the most frequent cover of the site, and are concentrated at peaks from 23 to 30 cm, and 23 to 40 cm above the general slope level (respectively).

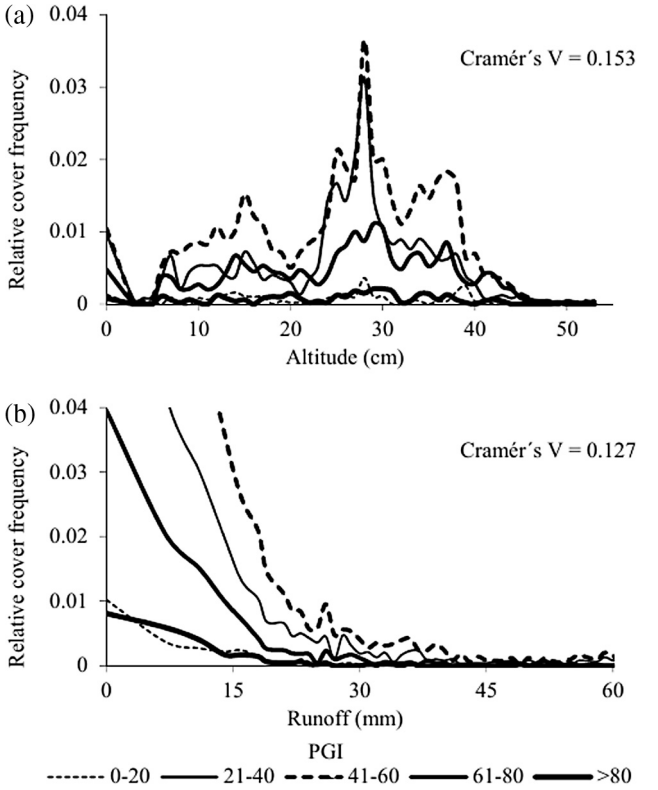

Fig. 2. High resolution imagery scale relations between (a) the vegetation cover frequency and terrain elevation and (b) vegetation cover frequency and potential runoff.

Regarding the cross-tabulation PRM × PCM (Fig. 2b), low values of potential runoff were observed in areas with both extremely sparse plant cover (PGI: >80) or extremely high (very dense shrubs) cover (PGI: 0–20).

3.2. Field sampling and experiments

The quantity of roots in soil, bulk density, K_{sat}, the average local slope (s^* and $s°$) and roughness of the soil surface (σ_s) measured at site B were significantly different in BS and VS plots (Table 1). The occurrence of mounds associated to plant patches resulted in higher s^* and σ_s values in VS as compared to BS patches. The bulk density measured at BS plots was higher than in the adjacent VS condition. K_{sat} values estimated at VS plots were significantly higher than those in BS plots.

K_{sat} estimates obtained through the TDI and the Wooding's (1968) model are greater (nearly twice as much) at the VS plots than those estimated based on textural data through ANN pedo-transfer functions (Fig. 3).

DS mean values (and consequent water ponding) (Rossi and Ares, 2012a) at VS plots were found to be higher than those estimated at BS inter-patches. *DS* is correlated with s^* (Fig. 4a). Also, $ç^*$ is negatively correlated to *DS* at BS inter-patches, and indifferent to variations in *DS* at VS plots (Fig. 4b).

Table 2 resumes the overland flow metrics estimated through the water flow experiments.

Fig. 5 shows a schematic lateral view of a patch area where differences in both overland and infiltration flow characteristics are shown as corresponding to the results of this study. Significant differences of micro-topography, water infiltration, saturated water conductivity, overland flow velocity, overland flow depth and

Table 1
Student's *t*-test of mean differences of soil properties at BS and VS conditions.

	$\bar{x}_{BS}$	$\bar{x}_{VS}$	*t* Value	*P*	*n*
SR (0–3 cm)	0.0278(±0.0047)	0.0501(±0.0079)	−2.589	0.012	60
SR (3–9 cm)	0.0402(±0.0042)	0.1028(±0.0137)	−4.945	0.000	60
SR (9–18 cm)	0.0464(±0.0039)	0.1029(±0.0194)	−3.789	0.001	60
Average *SR* (0–18 cm)	0.0381(±0.0023)	0.0966(±0.0125)	−5.738	0.000	60
SBD	1.511(±0.0791)	1.202(±0.0675)	2.980	0.003	25
K_{sat} (TDI)	0.0063(±0.0008)	0.0177(±0.0034)	−3.418	0.011	25
s^*	1.519(±0.357)	4.643(±0.830)	−3.558	0.001	25
s°	0.048(±0.009)	0.076(±0.007)	−2.386	0.013	25
σ_s	0.755(±0.307)	6.589(±2.293)	−2.625	0.008	25

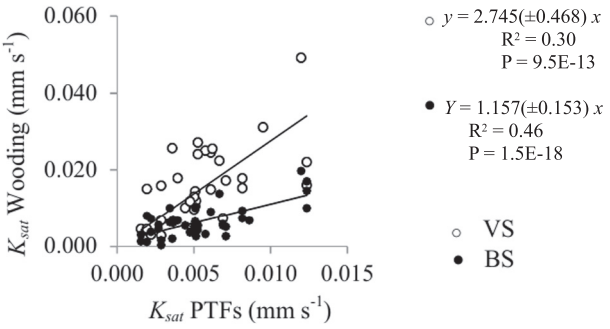

Fig. 3. Regression analysis between K_{sat} estimated by Pedotransference Functions (PTFs) and those estimated with the Tension Disk Infiltrometer (TDI) and Wooding's model. BS (black dots); VS (white dots).

depression storage were observed in vegetated patches as compared to BS inter-patches.

3.3. Spatial-explicit simulation of flow experiments

Fig. 6 shows examples of computer simulations with CREST solved at a high spatial resolution (*x*-*y*: 50 mm: *z*: 1 mm) with model parameters corresponding to the field area of micro-plot #19 (W: −64.98465; S: −42.2064333) in this study. This is a nearly "flat" plot with general slope −0.06° (NW to SE) and −0.2° from the center of the plant patch area in SW direction. CREST results of runoff flows are depicted overlaid on a rectified video scene of the plot at the end of a flow experiment and a map of contour lines. In order to enhance the visibility of local runoff flow paths, rainfall has been simulated to occur at restricted areas (red spots) inside and around the central vegetation patch, up- and downslope respect to it.

4. Discussion

4.1. Vegetation-topography-overland flow interactions

The association of low values of runoff with sites with extremely sparse plant cover or BS inter-patches (Fig. 2b) is in apparent contradiction with the well known observations (at landscapes with banded shrubs) that topographic slope can allow runoff from BS inter-patches to be collected as runon in vegetated patches (Reid et al., 1999; Traff et al., 2014). At spotted vegetation landscapes runoff generated at inter-patches could be routed onto the vegetated mounds provided it had sufficient momentum (proportional to the water depth and velocity). If not, the presence of mounds can cause water to run around them and not necessarily trap water and sediment in the shrub patches (Wilcox, 2003). The results shown at Fig. 2b fail to detect a mechanism that could route overland flow onto the vegetated mounds, as the potential energy gradients resulting from the topographic slope of the soil surface were not sufficient to account for such a path. Therefore the hypothesis (a) raised at the Introduction of this document (Section 1): "the low topographic slopes at the BS inter-patches may not give raise to the potential energy gradients sufficient to route overland flow onto the vegetated mounds" is not rejected.

The above mentioned results are in accordance with the vegetated mound residual genesis and maintenance hypothesis proposed for the Patagonian semiarid landscape at 1988 by Rostagno and Del Valle. According to this hypothesis, in the eventual scenario that runon flow would reach the patch border, runon water would not be trapped by the mound, but would erode it. Through evidences based on gravel pavement sampled at different positions within and around mounds near the study area, Rostagno and del Valle (1988) claim that the sides (or borders) of the mounds have been under the influence of a fluvial erosion rate. The authors claim that this fluvial erosion rate at the mound border

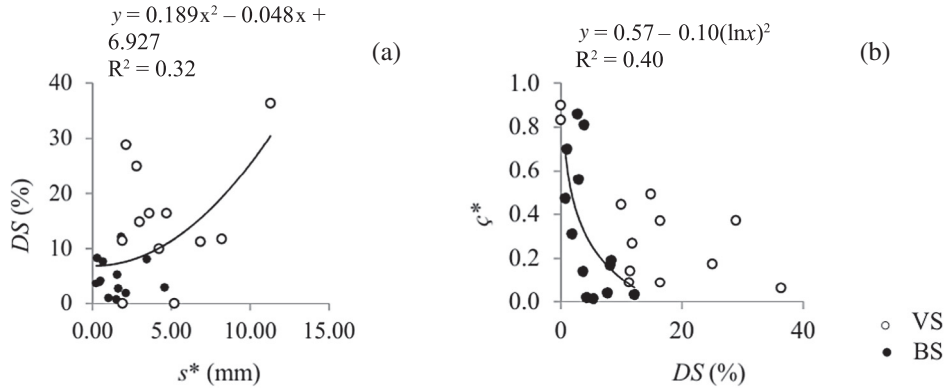

Fig. 4. Inter-plot relations between: (a) *DS*–s^* and b) $ç^*$–*DS* at BS (black dots) and VS (white dots).

Table 2
Means, confidence intervals and Student's *t*-test of mean differences of parameters and variables corresponding to BS ($n = 13$) and VS conditions ($n = 12$).

	$\bar{x}_{BS}$	$\bar{x}_{VS}$	*t* Value	*P*
$\hat{\varsigma}^*$	0.33(±0.08)	0.35(±0.081)	1.71	0.4316
$\hat{d}^*$	1.38(±0.51)	3.00(±0.77)	−1.78	0.0439[a]
DS	4.82(±0.93)	15.18(±3.09)	−3.31	0.0015[a]
ff	113.61(±39.30)	7.08(±2.33)	2.60	0.0081 [a]
Re	15.55(±8.08)	34.92(±10.42)	−1.48	0.0760 [b]
$V_{(s,W)}$	0.022(±0.007)	0.009(±0.003)	1.69	0.0514 [b]
$\hat{v}^*$	1.759(±0.572)	3.729(±0.672)	−2.24	0.0173[a]

[a] Mean differences significant ($P < 0.05$, *t* test).
[b] $\bar{x}_{BS}$ outside the range of $\bar{x}_{VS}$ ($P < 0.05$).

is greater than the erosion rate at the mound top (or center), but less than the erosion rates at the inter-mound. The mounds therefore are residual forms representing the original level of the ground. Here, mounds genesis and development is related to discrete shrub clumps that (a) shelter the underlying soil by dissipating the energy of the rain drops and preventing direct impact on the soil surface (Rostagno and del Valle, 1988), and (b) cause water to run around them and not necessarily deposit sediment in the under-shrub (Wilcox, 2003).

According to the results shown in Fig. 2a the most frequent plant patches (more or less dense shrubby-grass patches) occupy a range of mound altitude 20–40 cm above the general slope level, being the more dense plant forms (dense shrubby-grass patches) restricted to mounds from 23 to 30 cm above the general slope level. Considering the residual hypothesis of mound formation and maintenance of the study region, an average of 20–40 cm of topsoil has been eroded from the inter-mound area, after present vegetation cover was reached. These results agree with those of Rostagno and del Valle (1988) who measured 50 mound heights at a nearby site (30 × 30 m) with a slope less than 1%. The average height of the mounds at their survey was 41 cm. The highest and lowest individual mounds were 56 cm and 20 cm, respectively.

The hypothesis (b) proposed (Section 1) is not rejected with the results shown in Fig. 2b, as low values of potential runoff were observed in areas with high plant cover (PGI: 0–20). The low values of overland flow generated at the vegetation patch would propitiate it's retention (due to preferential infiltration and micro-topography) at the vegetation patch. The analysis of Fig. 2b only considers the topographic effects on overland flow, excluding the influence of high saturated hydraulic conductivity and micro-topography on the overland flow generated at the vegetated mound. This latter discussion will be expanded in Section 4.2 of this document.

4.2. Field sampling and experiments

4.2.1. Soil properties

The greater roughness of the soil surface in VS, as indicated by higher s^* and σ_s values, may result from the ground surface topography itself, or from vegetation structures (Martin et al., 2008). In a previous study on the overland flow generated from the plant patch areas of spotted vegetation (Rossi and Ares, 2016), the soil surface with greater proportion of roots was associated with positive correlations obtained between the average local slope (s^*) and roughness of the soil surface (σ_s).

As in Bochet et al. (1998), this higher abundance of roots (and organic matter) in the soil of vegetated patches as compared to BS inter-patches, is related to high bulk density values at the latter. In addition, high values of water conductivity observed in vegetation patches may result from macropore flow via root channels (Beven and Germann, 1982; Dong et al., 2003).

The high values of soil surface roughness and enhanced water conductivity observed in vegetation patches would propitiate the retention of the low overland flow generated (according to results of Fig. 2b) at the vegetated mound. The hypothesis (b) proposed (Section 1) is not rejected with these evidences.

Most K_{sat} (TDI) estimates in VS plots were higher than those obtained though the PTF estimates, a probable consequence of the omission of soil matrix information related to roots (Pritchett, 1991; Poesen and Lavee, 1994) in those latter.

4.2.2. Water flow experiments

Direct measurements of water fluxes (and the parameters that characterize them) at BS inter-patches and vegetated mounds

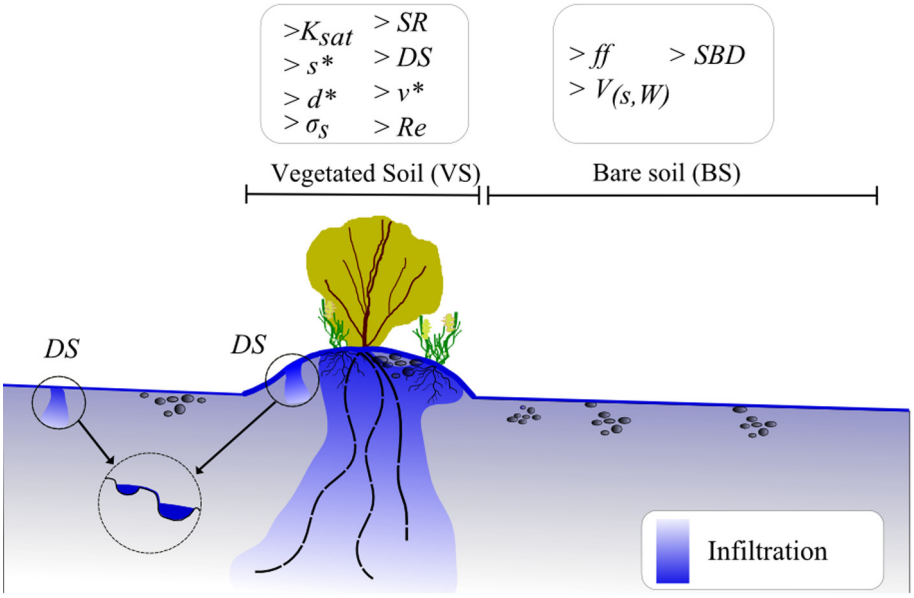

Fig. 5. Schematic summary of the hydrological effects of VS patches as inferred in this study. The changes of soil physical properties in patches and around them result in thin scale modifications of water infiltration, saturated water conductivity, overland flow velocity, overland flow depth, depression storage and the hydraulic characteristics of the overland flow.

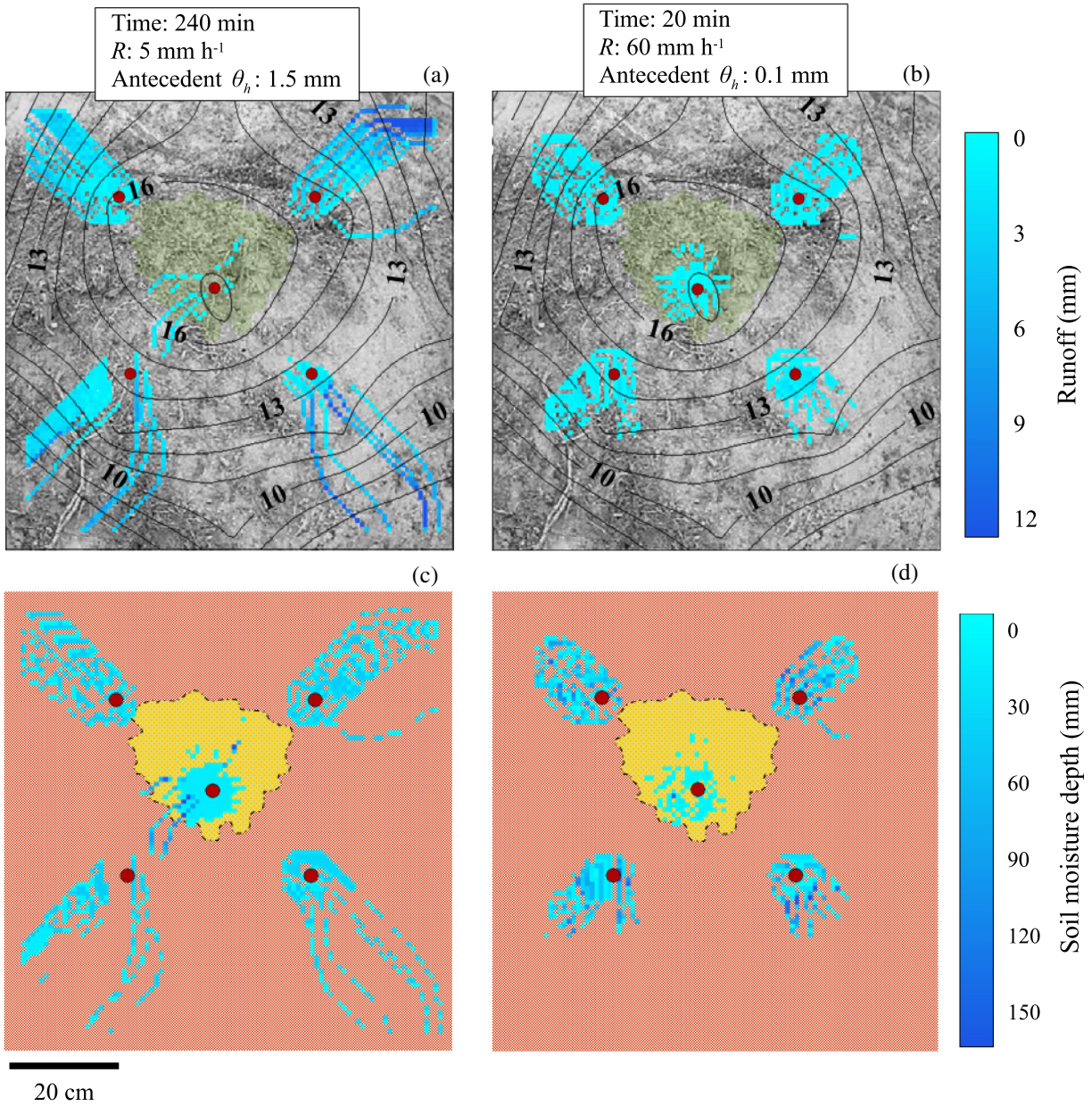

Fig. 6. Simulation results (CREST model) of (a and b) runoff flows (direction, flow depth) and (c and d) soil moisture depth resulting from local (red dots) rain inflows within and around plant patch areas at shallow-long storm as frequent during the Patagonian Winter (a and c) and deep-and-short rainfall event, as is usual during the Patagonian Summer (b and d). Runoff results are overlaid on a video scene of the plot and a map of contour lines (mm). (For interpretation of the references to colour in this figure legend, the reader is referred to the web version of this article.)

was feasible through the experimental setup here applied. The method accurately reproduced runoff and infiltration conditions at previous works (Rossi and Ares, 2012a, 2016) where the hydrological estimates have been analyzed and compared with other similar semi-arid hydrological plot model estimates.

The spatial distribution of water at the end of the flow experiments can be interpreted as resulting from the combined effects of enhanced K_{sat} at VS and micro-topographic characteristics (slope, roughness) of BS and VS plots as described in Table 1. At comparable water inflow rates at VS and BS the RP velocities (v^*) were higher at VS plots. Nevertheless, the enhanced infiltration in VS plots extracts water that would otherwise flow overland. This results in lower overland flow velocities corrected by slope and inflow rate ($V(s,W)$).

Higher mean values of d^* at VS plots are consistent with their higher surface roughness (see σ_s, Table 1) resulting from the presence of plant stems and their disturbing effect on the soil surface (Dunne et al., 1991; Jin et al., 2000).

Re numbers in the field flow experiments were in a low range (<50) where predominant laminar flow can be assumed, although the geometry of the flow paths is undefined due to micro-topography and vegetation obstructions. *Re* were higher at VS than at BS as a probable consequence of deeper flow streams (see d^* above) and consequently diminished flow resistance (Dunkerley, 2001).

Friction factor (*ff*) was estimated (Eq. (11)) assuming laminar flow because the flow of the field flow experiments presented low *Re* values (Eq. (10), Table 2). Mean *ff* values were significantly higher at BS than at VS plots as a probable consequence of deeper flow streams in these latter. In classical flow experiments at large field plots Abrahams et al. (1990) observed a general tendency of friction to decrease with increasing overland flow depth.

DS mean values (and consequent water ponding) (Rossi and Ares, 2012a) and σ_s at VS plots were found to be higher than those estimated at BS inter-patches. High *DS* and σ_s mean values obtained in the VS plots would contribute to retain the overland flow generated inside the plant patch (originated by stemflow and throughfall, Rossi and Ares, 2016) as these patch attributes contribute to several aspects of resistance to overland flow (Martin et al., 2008). Rossi and Ares (2012a) raised the point that saturated infiltration should be assumed to occur at *DS* areas, which would further reduce the quantity of water available to overland flow. The hypothesis (b) proposed (Section 1) is not rejected with these evidences.

The positive correlation found between *DS* and s^* at the vegetated mounds (Fig. 4a) is consistent with findings of studies of Huang and Bradford (1990) who observed that water storage in depressions increases as the topography variability increases. When considering this positive correlation it could be assumed that steep vegetated mounds would be more likely to retain the overland flow generated inside the plant patch than mounds with a small slope. However, the increase of *DS* with mound slope does not imply that runoff becomes greater with smaller slopes as the mean runoff coefficient ($ç^*$) is indifferent to variations in *DS* (Fig. 4b). This is probably due to the combined effect of fast preferential infiltration flow caused by macropores and root channels and reduced overland flow through high roughness.

As runon water generated at BS inter-patches reaches a border of a vegetated mound, redistribution of this water would be obstructed by the high values of *DS* (and water ponding) and σ_s. This runon water retained at the patch border would feed the infiltration flow. If the runon had enough depth (due to ponding or deep overland flow) to inundate the mound (or a portion of it) this would imply a free surface of water that would feed the infiltration flow. Nevertheless, unless the ponding depth became enough to inundate the entire mound, infiltration flow due to runon would be limited only on that portion of the vegetated mound. This would not support the use of invariant infiltration flows throughout mound areas when simulating thin-scale hydrological processes in spotted vegetation areas.

$ç^*$ at BS inter-patches is negatively correlated to *DS* (Fig. 4b); such as is usually assumed in modeling studies (Takken et al., 2001; Darboux et al., 2002a,b; Abedini et al., 2006). Similarly, Muñoz-Robles et al. (2011) found that in the inter-patches at semiarid south-eastern Australia, the average runoff rate was negatively correlated with surface roughness.

4.3. Water fluxes between BS and the plant patch at typical Patagonian storms

As graphically resumed in Fig. 5, vegetated mounds modify several edaphic and hydrological characteristics at thin (<1 m) spatial scales. Significant differences of micro-topography, water infiltration, saturated hydraulic conductivity, overland flow velocity, overland flow depth and depression storage were observed in vegetated mounds as compared to BS inter-patches. High micro-topographic roughness and *DS*, thickened overland flow depth and decreased flow friction occurred at the vegetated mound. At BS plots prevailing low slopes and *DS* were found to be important variables attenuating the surface runoff. Thompson's et al. (2011) numerical experiments on flat sites in patchy arid ecosystems suggest that the infiltration contrast between VS patches and BS inter-patches can induce significant lateral transport of water during storm events. Moreover, they argue that the nature of the infiltration contrast is the most significant control on the lateral transport of water, with the surface roughness acting as a secondary effect. These modeling results are consistent with the field observations made in this study regarding the significant differences of surface roughness between vegetated mounds and BS inter-patches; which would likely impede lateral redistribution, or at least confine redistribution strongly to the edges of vegetated mounds.

Both, Winter and Summer rainfall scenarios simulated (Fig. 6) considered the influence of varying hydraulic conductivity with micro-topography. Fig. 6a and c shows the distribution of predominantly Hewlettian flows during a shallow-long storm as frequent during the Patagonian Winter. Storms during this season usually occur on soils with relative high moisture at the top of the soil profile. It is observed (Fig. 6a) that overland flow from the plant patch diverge from it and extend over the surrounding BS area, while runoff from outside the plant patch tend to diverge from it and follow the (small) topographic gradient. Overland flow depths resulted greater at the BS inter-patch near the edge of the mound than under the plant patch (where more roots were sampled), indicating the occurrence of a thin layer (up to 12 mm) of water ponding. This overland flow depth was not enough to reach and inundate the area under the plant patch or the area under most plant patches of the study region that occupy a range of mound altitude 20–40 cm above the general slope level.

An inspection of the model output corresponding to the spatial distribution of the accumulated moisture below the soil surface (Fig. 6c) indicates that the soil under the plant patches accumulated more moisture and reaches saturation long before this occurs in BS surrounding areas. In this scenario the vegetation patch obstructed the runoff from the BS surroundings, but this water flow was not reinfiltrated as runon under the plant canopy; instead it was infiltrated at the BS inter-patch, near the edge of the mound. Nevertheless, the BS inter-patch accumulated less soil moisture as compared with the vegetated area because the infiltration rate at this region was lower compared to the plant canopy.

The situation is similar when considering predominantly Hortonian runoff flows following a deep-and-short rainfall event on nearly dry soil (Fig. 6b and d), as is usual during the Patagonian Summer. As in typical winter condition, the soil under the plant patches also accumulates more moisture and reaches saturation long before this occurs in BS inter-patch surrounding areas.

Regarding the hypothesis (b), the overland flow generated inside the vegetation patch was effectively retained at the Summer rainfall scenario; while at the Winter rainfall scenario two threads of 6.7 cm of runoff were routed outside the plant patch. Therefore this hypothesis is not rejected concerning the Summer rainfall, though rejected in the case of the Winter rainfall event.

Overland flow depths at the BS inter-patches are deeper at the Winter scenario compared to the Summer scenario. Therefore during an extremely long winter storm or with high antecedent soil moisture conditions it is more likely that ponding may occur at the inter-patch and reach the plant patch border with high infiltration rates. In this scenario infiltration rate would increase as the mound becomes submerged under the greater runoff or ponding depth (Fox et al., 1998). However the modeling results here shown at typical rainfall scenarios fail to detect a contrast in infiltration rate enough to lead to a free-surface gradient in ponded water that could route overland flow onto the vegetation-related mound and inundate it. Therefore through these results the hypothesis (c) (Section 1) is not rejected.

5. Conclusions

The results here obtained at a high resolution imagery scale, field observations and thin scale modeling do not support the hypothesis of generalized fluvial transport from BS inter-patches to vegetated mounds in relatively flat spotted semiarid landscapes. Local slopes at BS inter-patches were not sufficient to route flow onto the vegetated mounds either at the Winter or Summer rainfall

scenarios. Also, depression storage was found to be an important variable attenuating the surface runoff at the water flow experiments. It is more likely that ponding may occur at the inter-patch that could reach the plant patch border with high infiltration rates during an extremely long winter storm or with high antecedent soil moisture conditions. Overland flow and infiltration were found to be spatially variable and associated with plant cover, vegetation-related mounds, depressions and micro-topography. *DS* mean values (and consequent water ponding) at vegetated mounds were found to be higher than those estimated at BS inter-patches. At BS inter-patches, prevailing low slopes and *DS* were found to be important variables attenuating the surface runoff. These results are in accordance with the vegetated mound genesis hypothesis proposed for the Patagonian semiarid landscape and have implications on resource redistribution and management.

Acknowledgments

We thank the editors and anonymous reviewers for their suggestions in improving the manuscript. This study was supported by grants of Agencia Nacional de Investigaciones Científicas y Técnicas (ANPCyT) PICT13-1368 and PICT 15-3658.

Appendix A. Supplementary material

Supplementary data associated with this article can be found, in the online version, at http://dx.doi.org/10.1016/j.jhydrol.2017.01.016.

References

Abedini, M.J., Dickinson, W.T., Rudra, R.P., 2006. On depressional storages: the effect of DEM spatial resolution. J. Hydrol. 318 (1–4), 138–150.
Abraham, E., del Valle, H., Roig, F., Torres, L., Ares, J., Coronato, F., Godagnone, R., 2009. Overview of the geography of the Monte desert of Argentina. J. Arid Environ. 73, 144–153.
Abrahams, A.D., Parsons, A.J., Luk, S.H., 1990. Field experiments on the resistance to overland flow on desert hillslopes. Erosion, Transport and Deposition Processes, in: Proceedings of the Jerusalem Workshop, IAHS Publ. no. 189, Jerusalem.
Appels, W.M., Bogaart, P.W., van der Zee, S.E.A.T.M., 2016. Surface runoff in flat terrain: how field topography and runoff generating processes control hydrological connectivity. J. Hydrol. 534, 493–504.
Ares, J.O., Beeskow, A.M., Bertiller, M.B., Rostagno, M., Irisarri, M., Anchorena, J., Defossé, G.E., Merino, C.A., 1990. Structural and dynamic characteristics of overgrazed lands of northern Patagonia, Argentina. In: Breymeyer, A. (Ed.), Managed Grasslands: Regional Studies, pp. 149–175.
Ares, J.O., del Valle, H., Bisigato, A., 2003. Detection of process-related changes in plant patterns at extended spatial scales during early dryland desertification. Glob. Chang. Biol. 9, 1643–1659.
Bedford, D.R., Small, E.E., 2008. Spatial patterns of ecohydrologic properties on a hillslope–alluvial fan transect, central New Mexico. Catena 73, 34–48.
Bertiller, M.B., Beeskow, A.M., Coronato, F., 1991. Seasonal environmental variation and plant phenology in arid Patagonia (Argentina). J. Arid Environ. 21, 1–11.
Beven, K., Germann, P., 1982. Macropores and water flow in soil. Water Resour. Res. 18, 1311–1325.
Bisigato, A.J., Bertiller, M.B., 1999. Seedling emergence and survival in contrasting soil microsites in Patagonian Monte shrubland. J. Veg. Sci. 10 (3), 335–342.
Bochet, E., Poesen, J., Rubio, J.L., 2006. Runoff and soil loss under individual plants of a semiarid Mediterranean shrubland: influence of plant morphology and rainfall intensity. Earth Surf. Process. Landf. 31, 536–549.
Bochet, E., Poesen, J., Rubio, J.L., 2000. Mound development as an interaction of individual plants with soil, water erosion and sedimentation processes on slopes. Earth Surf. Process. Landf. 25, 847–867.
Bochet, E., Rubio, J.L., Poesen, J., 1998. Relative efficiency of three representative matorral species in reducing water erosion at the microscale in a semi-arid climate (Valencia, Spain). Geomorphology 23, 139–150.
Böhm, W., 1979. Methods of Studying Root Systems. Springer Verlag, Berlin.
Bromley, J., Brouwer, J., Barker, A.P., Gaze, S.R., Valentin, C., 1997. The role of surface water redistribution in an area of patterned vegetation in a semi-arid environment, south-west Niger. J. Hydrol. 198, 1–29.
Bryan, R.B., Brun, S.E., 1999. Laboratory experiments on sequential scour/deposition and their application to the development of banded vegetation. Catena 37 (1–2), 147–163.
Caldwell, T.G., Young, M.H., Zhu, J., McDonald, E.V., 2008. Spatial structure of hydraulic properties from canopy to interspace in the Mojave Desert. Geophys. Res. Lett. 35. http://dx.doi.org/10.1029/2008GL035095.
Cammeraat, L.H., Imeson, A.C., 1999. The evolution and significance of soil-vegetation patterns following land abandonment and fire in Spain. Catena 37, 107–127.
Campanella, M.V., Rostagno, C.M., Videla, L.S., Bisigato, A.J., 2016. Interacting effects of soil degradation and precipitation on plant productivity in NE Patagonia, Argentina. Arid Land Res. Manage. 30 (1), 79–88.
Carrera, A.L., Bertiller, M.B., Larreguy, C., 2008. Leaf litter fall, fine root production, and decomposition in shrublands with different canopy structure induced by grazing in the Patagonian Monte, Argentina. Plant Soil 311, 39–50.
Cerdá, A., 1997. The effect of patchy distribution of *Stipa tenacissima* L. on runoff and erosion. J. Arid Environ. 9, 27–38.
Chen, L., Sela, S., Svoray, T., Assouline, S., 2013. The role of soil-surface sealing, microtopography, and vegetation patches in rainfall-runoff processes in semiarid areas. Water Resour. Res. 49 (9), 5585–5599.
Chu, X., Yang, J., Chi, Y., Zhang, J., 2013. Dynamic puddle delineation and modeling of puddle to-puddle filling-spilling-merging-splitting overland flow processes. Water Resour. Res. http://dx.doi.org/10.1002/wrcr.20286.
Cornet, A.F., Montaña, C., Delhoume, J.P., Lopez-Portillo, J., 1992. Water flows and dynamics of desert vegetation stripes. In: Hansen, A.J., di Castri, F. (Eds.), Landscape Boundaries—Consequences for Biotic Diversity and Ecological Flows. Springer-Verlag, New York, pp. 327–345.
Darboux, F., Gascuel-Odoux, C., Davy, P., 2002a. Effects of surface water storage by soil roughness on overland-flow generation. Earth Surf. Process. Landf. 17 (3), 223–233.
Darboux, F., Davy, P., Gascuel-Odoux, C., 2002b. Effect of depression storage capacity on overland-flow generation for rough horizontal surfaces: water transfer distance and scaling. Earth Surf. Process. Landf. 27, 177–191.
Deblauwe, V., Couteron, P., Bogaert, J., Barbier, N., 2011. Determinants and dynamics of banded vegetation pattern migration in arid climates. Ecol. Monogr. 82, 3–21.
del Valle, H.F., Elissalde, N.O., Gagliardini, D.A., Milovich, J., 1998. Status of desertification in the Patagonian region: assessment and mapping from satellite imagery. Arid Soil Res. Rehabil. 12, 95–122.
Dingman, S.L., 2007. Analytical derivation of at-a-station hydraulic– geometry relations. J. Hydrol. 334, 17–27.
Dong, W., Yu, Z., Weber, D., 2003. Simulations on soil water variation in arid regions. J. Hydrol. 275 (3–4), 162–181.
Dunkerley, D.L., 2001. Estimating the mean speed of laminar overland flow using dye-injection-uncertainty on rough surfaces. Earth Surf. Process. Landf. 26, 363–374.
Dunkerley, D.L., 2002. Infiltration rates and soil moisture in a groved mulga community near Alice Springs, arid central Australia: evidence for complex internal rainwater redistribution in a runoff-runon landscape. J. Arid Environ. 51 (2), 199–219.
Dunkerley, D.L., 2003. Determining friction coefficients for interrill flows: the significance of flow filaments and backwater effects. Earth Surf. Process. Landf. 28 (5), 475–491.
Dunkerley, D.L., Brown, K.J., 1995. Runoff and runon areas in a patterned chenopod shrubland, arid western New SouthWales, Australia: characteristics and origin. J. Arid Environ. 30, 41–55.
Dunne, T., Zhang, W., Aubry, B.F., 1991. Effects of rainfall, vegetation and microtopography on infiltration and runoff. Water Resour. Res. 27, 2271–2285.
Fox, D.M., Bissonnais, Y.L., Quetin, P., 1998. The implications of spatial variability in surface seal hydraulic resistance for infiltration in a mound and depression microtopography. Catena 32, 101–114.
Frei, S., Fleckenstein, J.H., 2014. Representing effects of micro-topography on runoff generation and sub-surface flow patterns by using superficial rill/depression storage height variations. Environ. Model. Softw. 52, 5–18.
Gee, G.W., Bauder, J.W., 1986. Particle-size analysis. In: Klute, A. (Ed.), Methods of Soil Analysis, Part 1, Physical and Mineralogical Methods, second Ed., Agronomy Monograph No. 9, ASA-SSSA.
Harman, C., Lohse, K., Troch, P.A., Sivapalan, M., 2014. Spatial patterns of vegetation, soils, and microtopography from terrestrial laser scanning on two semiarid hillslopes of contrasting lithology. J. Geophys. Res. http://dx.doi.org/10.1002/2013JG002507.
Huang, C., Bradford, J.M., 1990. Depressional storage for Markov-Gaussian surfaces. Water Resour. Res. 26, 2235–2242.
ISO 11272, 1998. Deutsches Institut für Normung –Soil Quality – Determination of Dry Bulk Density, Beuth Verlag, Berlin.
Jenson, S., Domingue, J., 1988. Extracting topographic structure from digital elevation data for geographic information system analysis. Photogramm. Eng. Rem. Sens. 54 (11), 1593–1600.
Jin, C.X., Romkens, M.J.M., Griffioen, F., 2000. Estimating Manning's roughness coefficient for shallow overland flow in non- submerged vegetative filter strips. Trans. ASAE 43 (6), 1459–1466.
Li, X., Contreras, S., Solé-Benet, A., 2008. Unsaturated hydraulic conductivity in limestone dolines: influence of vegetation and rock fragments. Geoderma 145 (3–4), 288–294.
Liu, H., Zhao, W., He, Z., 2013a. Self-organized vegetation patterning effects on surface soil hydraulic conductivity: a case study in the Qilian Mountains, China. Geoderma 192, 362–367.
Liu, Y., Fu, B., Lü, Y., Gao, G., Wang, S., Zhou, J., 2013b. Linking vegetation cover patterns to hydrological responses using two process-based pattern indices at the plot scale. Sci. China Earth Sci. 56 (11), 1888–1898.
Ludwig, J.A., Tongway, D.J., Marsden, S.G., 1999. Stripes, strands or stipples: modelling the influence of three landscape banding patterns on resource capture and productivity in semi-arid woodlands, Australia. Catena 37, 257–273.

Ludwig, J.A., Wilcox, B.P., Breshears, D.D., Tongway, D.J., Imeson, A.C., 2005. Vegetation patches and runoff-erosion as interacting ecohydrological processes in semiarid landscapes. Ecology 86, 288–297.
Martin, Y., Valeo, C., Tait, M., 2008. Centimetre-scale digital representations of terrain and impacts on depression storage and runoff. Catena 75 (2), 223–233.
Mayor, A.G., Bautista, S., Small, E.E., Dixon, M., Bellot, J., 2008. Measurement of the connectivity of runoff source areas as determined by vegetation pattern and topography: a tool for assessing potential water and soil losses in drylands. Water Resour. Res. 44 (10). http://dx.doi.org/10.1029/2007WR006367.
Mazzonia, E., Vazquez, M., 2009. Desertification in Patagonia. Dev. Earth Surf. Proces. 13, 351–377.
Moreno-de las Heras, M., Pérez-Domingo, S., Espigares, T., Nicolau, J.M., 2012. Hydrological heterogeneity in Mediterranean reclaimed slopes: runoff and sediment yield at the patch and slope scales along a gradient of overland flow. Hydrol. Earth Syst. Sci. 16 (5), 1305–1320.
Mügler, C., Planchon, O., Patin, J., Weill, S., Silvera, N., Richard, P., Mouche, E., 2011. Comparison of roughness models to simulate overland flow and tracer transport experiments under simulated rainfall at plot scale. J. Hydrol. 402 (1), 25–40.
Muñoz-Robles, C., Reid, N., Tighe, M., Briggs, S.V., Wilson, B., 2011. Soil hydrological and erosional responses in patches and inter-patches in vegetation states in semi-arid Australia. Geoderma 160 (3–4), 524–534.
Nakayama, Y., Boucher, R.F., 1998. Introduction to Fluid Mechanics, Chapter 4. Butterworth-Heinemann, Oxford.
Nicolau, J.M., Sole, A., Puigdefabregas, J., Gutierrez, L., 1996. Effects of soil and vegetation on runoff along a catena in semi-arid Spain. Geomorphology 14, 297–309.
Parsons, A.J., Abrahams, A.D., Wainwright, J., 1994. On determining resistance to interrill overland flow. Water Resour. Res. 30, 3515–3521.
Poesen, J., Lavee, H., 1994. Rock fragments in top soils: significance and processes. Catena 23, 1–28.
Pritchett, W.L., 1991. Suelos Forestales. Propiedades, conservación y mejoramiento, LIMUSA, Grupo Noriega Editores, Mexico, D.F.
Puigdefábregas, J., Solé-Benet, A., Gutierrez, L., Barrio, G., Boer, M., 1999. Scales and processes of water and sediment redistribution in drylands: results from the Rambla Honda field site in southeast Spain. Earth Sci. Rev. 48, 39–70.
Reid, K.D., Wilcox, B.P., Breshears, D.D., MacDonald, L., 1999. Runoff and erosion in a piñon–juniper woodland: influence of vegetation patches. Soil Sci. Soc. Am. J. 63, 1869–1879.
Rodríguez-Caballero, E., Cantón, Y., Lazaro, R., Solé-Benet, A., 2014. Cross-scale interactions between surface components and rainfall properties. Non-linearities in the hydrological and erosive behavior of semiarid catchments. J. Hydrol. 517, 815–825.
Rossi, M.J., Ares, J.O., 2012a. Depression storage and infiltration effects on overland flow depth-velocity-friction at desert conditions: field plot results and model. Hydrol. Earth Syst. Sci. 16 (9), 3293–3307.
Rossi, M.J., Ares, J.O., 2012b. Close range stereophotogrammetry and video imagery analyses in soil ecohydrology modelling. Photogramm. Rec. 27, 111–126.
Rossi, M.J., Ares, J.O., 2016. Overland flow from plant patches: coupled effects of preferential infiltration, surface roughness and depression storage at the semiarid Patagonian Monte. J. Hydrol. 533, 603–614.
Rostagno, C.M., Del Valle, H.F., 1988. Mounds associated with shrubs in aridic soils of northeastern Patagonia: characteristics and probable genesis. Catena 15, 347–359.
Rostagno, C.M., Del Valle, H.F., Videla, L., 1991. The influence of shrubs on some chemical and physical properties of an aridic soil in north-eastern Patagonia, Argentina. J. Arid Environ. 20, 179–188.
Saco, P.M., Willgoose, G.R., Hancock, G.R., 2007. Ecogeomorphology of banded vegetation patterns in arid and semi-arid regions. Hydrol. Earth Syst. Sci. 11, 1717–1730.
Sala, O.E., Golluscio, R.A., Lauenroth, W.K., Soriano, A., 1989. Resource partitioning between shrubs and grasses in the Patagonian steppe. Oecologia 81, 501–505.
Schaap, M.G., Leij, F.J., 1998. Database related accuracy and uncertainty of pedotransfer functions. Soil Sci. 163, 765–779.
Stephens, M.A., 1970. Use of the Kolmogorov-Smirnov, Cramer-Von Mises and related statistics without extensive tables. J. R. Statist. Soc. B 32, 115–122.
Strohmeier, S.M., Nouwakpo, S.K., Huang, C.H., Klik, A., 2014. Flume experimental evaluation of the effect of rill flow path tortuosity on rill roughness based on the Manning-Strickler equation. Catena 118, 226–233.
Takken, I., Govers, G., Jetten, V., Nachtergaele, J., Steegen, A., Poesen, J., 2001. Effects of tillage on runoff and erosion patterns. Soil Tillage Res. 61, 55–60.
Tarboton, D.G., 1997. A new method for the determination of flow directions and upslope areas in grid digital elevation models. Water Resour. Res. 33, 309–319.
Thompson, S., Katul, G., Konings, A., Ridolfi, L., 2011. Unsteady overland flow on flat surfaces induced by spatial permeability contrasts. Adv. Water Resour. 34 (8), 1049–1058.
Traff, D.C., Niemann, J.D., Middlekauff, S.A., Lehman, B.M., 2014. Effects of woody vegetation on shallow soil moisture at a semiarid montane catchment. Ecohydrology 947, 935–947.
van Genuchten, M.T., 1980. A closed-form equation for predicting the hydraulic conductivity of unsaturated soils. Soil Sci. Soc. Am. J. 47 (44), 892–898.
Wang, X.P., Wang, Z.N., Berndtsson, R., Zhang, Y.F., Pan, Y.X., 2011. Desert shrub stemflow and its significance in soil moisture replenishment. Hydrol. Earth Syst. Sci. 15 (2), 561–567.
Wilcox, B.P., 2003. Runoff from rangelands: the role of shrubs. In: McGinty, A., Hanselka, C.W., Ueckert, D.N., Hamilton, W., Lee, M. (Eds.), Shrub Management. Texas A&M University, College Station, Texas.
Wilcox, B.P., Breshears, D.D., Allen, C.D., 2003. Ecohydrology of are- source-conserving semiarid woodland: effects of scale and disturbance. Ecol. Monogr. 73, 223–239.
Wooding, R.A., 1968. Steady infiltration from a shallow circular pond. Water Resour. Res. 4, 1259–1273.
Wu, G.L., Wang, D., Liu, Y., Hao, H., Fang, N., Shi, Z., 2016. Mosaic-pattern vegetation formation and dynamics driven by the water-wind crisscross erosion. J. Hydrol. 538, 355–362.